Available online at www.sciencedirect.com
SCIENCE DIRECT
Catalysis Today 99 (2005) 309–314
CATALYSIS TODAY
www.elsevier.com/locate/cattod

Physico-chemical characterization and catalysis on SBA-15 supported molybdenum hydrotreating catalysts

G. Murali Dhar[a,*], G. Muthu Kumaran[a], Manoj Kumar[a], K.S. Rawat[a], L.D. Sharma[a], B. David Raju[b], K.S. Rama Rao[b]

[a]*Indian Institute of Petroleum, Dehradun 248005, India*
[b]*Indian Institute of Chemical Technology, Hyderabad 500007, India*

Available online 28 December 2004

Abstract

SBA-15 supported Mo, CoMo, NiMo catalysts were prepared. The supports were characterized by surface area, pore size distribution, and X-ray diffraction. The finished catalysts in oxide state were characterized by surface area analysis and X-ray diffraction in the region where the molybdenum oxide lines are seen. The sulfided catalysts were examined by oxygen chemisorption at low temperatures. The catalytic functionalities of these catalysts viz hydrodesulfurization (HDS) and hydrogenation were evaluated on sulfided catalysts. The catalytic activities of these catalysts are compared with γ-Al_2O_3- and SiO_2-supported catalysts. An attempt is made to understand the relationship between oxygen chemisorption and catalytic activities with the help of other characterization results.

Keywords: CoMo catalysts; SBA-15; Oxygen chemisorption; Hydrotreating catalysts

1. Introduction

Fuel cell systems are receiving increasing attention worldwide as efficient and environmental friendly energy options especially for automotive applications. Hydrocarbon fuels such as gasoline and diesel are promising fuels for production of syngas and hydrogen for fuel cells at the required site. However, they often contain sulfur compounds that are poisons to the catalysts and electrodes that are used in fuel cell setup [1].

Several types of fuel cells are at various stages development. Based on the type of electrode used, fuel cells are divided into five types. These are alkaline fuel cells (AFC), proton exchange membrane fuel cells (PEMFC), phosphoric acid fuel cells (PAFC), molten carbonate fuel cells (MCFC), and solid oxide fuel cells (SOFC). All the fuel cells require fuels with sulfur level less than few ppm. For example PAFC fuel cells require fuels with sulfur around 50 ppm. While MCFC requires sulfur less than 0.5 ppm and SOFC requires around 1 ppm. PEMFC's demand most stringent sulfur specifications of less than 0.1 ppm levels. It appears whatever may be the fuel cell option one considers, sulfur level in fuels need to be brought down to few ppm level [1,2].

Developments in petroleum refining are moving in that direction to produce clean fuels with sulfur below 50 ppm. However, to go to 0.1 ppm level is a challenging task. Calculations indicated that to bring sulfur level from present 500 ppm to 0.1 ppm level needs catalysts, which are ~7 times more active than existing ones [2]. The enormity of the task can be understood, if one realizes in past two decades only incremental improvements of catalysts were possible inspite of intensive research in highly competitive situation. Therefore, focused research is required to achieve such a challenging goal. There are many approaches to prepare better catalysts to meet these challenges, like changing the active component, varying the preparation method and changing the supports etc. Wide variety of materials have been used as supports in an attempt to increase the activity. These include clays [3], zeolites [4,5], oxides like SiO_2 [6], TiO_2 [7], ZrO_2 [8], MgO [9], and carbon [10]. Several combinations of mixed oxides like SiO_2–Al_2O_3 [11], SiO_2–

* Corresponding author. Fax: +91 135 660202.
E-mail address: gmurli@iip.res.in (G.M. Dhar).

0920-5861/$ – see front matter © 2004 Published by Elsevier B.V.
doi:10.1016/j.cattod.2004.10.005

TiO_2 [12], SiO_2–ZrO_2 [13], ZrO_2–TiO_2 [14,3], TiO_2–Al_2O_3 [15–18] have been studied with great interest [19]. In recent times the attention is shifted to zeolites like Y, USY, and mesoporous materials like MCM-41 [20–23], HMS [24,4,5], SBA-15 [25], mesoporous Al_2O_3 [26] systems. MCM-41 supported CoMo catalysts are reported to exhibit higher activities for conversion of benzothiophene and petroleum residues. Song and Reddy [27] demonstrated that CoMo/MCM-41 is substantially more active than CoMo/γ–Al_2O_3 catalysts at high molybdenum loadings. Chiranjeevi et al. [24,28] reported that Al-HMS materials based CoMo, NiW catalysts showed superior activities compared γ-Al_2O_3-supported catalysts. Highly active MoS_2 catalysts supported on Mesoporous Al_2O_3 were reported by Zadrazil and coworkers [26]. Vradman et al. [25] reported higher activites for HDS and hydrogenation using Ni-W-S/SBA-15 catalysts. In this investigation we are reporting a detailed systematic study on Mo, CoMo, NiMo supported on siliceous SBA-15.

2. Experimental

SBA-15 was prepared by the following published procedure using a tri-block Poly (ethylene oxide) Poly (propylene oxide) Poly (ethylene oxide) polymer as structure directing agent [29]. In a typical preparation the required amount of tri-block polymers is dispersed in distilled water and the resultant solution is mixed with required amount of HCl. Finally required amount tetra ethyl ortho silicate is added drop-wise. The mixture is stirred for 12 h at 40 °C. The above said solution is transferred to Teflon bottle and aged at autogenous pressure for 12 h at 80 °C. The material obtained after filtration was dried at 110 °C for 6 h and calcined at 500 °C for 2 h. The BET surface area was found to be 696 m^2/g. The calcined mesoporous materials were characterized by X-ray diffraction (XRD) using GE XRD-6 diffractometer and micromeritics ASAP-2010 adsorption–desorption unit. The Al_2O_3 support was prepared by homogeneous precipitation method using urea at 90 °C.

The molybdenum-supported catalysts were prepared by incipient wetness impregnation method using appropriate concentrations of ammonium hepta molybdate using SBA-15 material as the support. The Co- or Ni-promoted catalysts were prepared by impregnating the promoter on an oven dried Mo supported catalysts. The impregnated catalysts were dried in air at 100 °C over night and all the catalysts were calcined at 500 °C for 5 h.

The oxygen uptakes were measured at −78 °C in a conventional high vacuum system, on a catalyst sulfided at 400 °C for 2 h using a CS_2/H_2 mixture at a flow rate of 40 ml/min, according to double isotherm procedure reported by Parekh and Weller [30] for reduced molybdenum catalysts. The same system was used for the BET surface area measurements. The thiophene HDS, cyclohexene HYD were carried out at 400 °C on a catalyst sulfided at the same temperature for 2 h in flow of CS_2/H_2 mixture, in a fixed-bed reactor operating at atmospheric pressure and interfaced with a six-way sampling valve for product analysis [31]. First order rates were evaluated according the equation $x = r(W/F)$ where r is rate in moles per hour per gram, x the fractional conversion, W the weight of the catalyst in grams, and F is flow rate of the reactant in moles per hour [7,31]. The conversions were kept (below 15%) to avoid diffusional limitations.

3. Results and discussion

3.1. Characterization of the support

The support obtained by procedure described in experimental section was characterized by BET surface area, BJH pore size distribution, and X-ray diffraction methods in order to confirm that the product obtained is indeed SBA-15 of suitable physico-chemical properties. The BET surface area of the support was found to be 696 m^2/g. The mesopore distribution is sharp around 72 Å (Fig. 1). The XRD patterns (Fig. 2) of the support indicated sharp peaks in low angle region around 90 Å d spacing characteristic of SBA-15 materials. There were also small peaks around 54.04, 46.52 Å d spacing. The XRD and pore size distribution data agreed with those reported in literature [29]. The XRD, pore size distribution, and surface area confirmed that the synthesized support material is indeed SBA-15.

3.2. Characterization of the catalysts

3.2.1. Surface area

The molybdenum catalysts prepared by incipient wetness impregnation and subsequent calcinations at 500 °C for 5 h were examined by BET surface area, X-ray diffraction, and

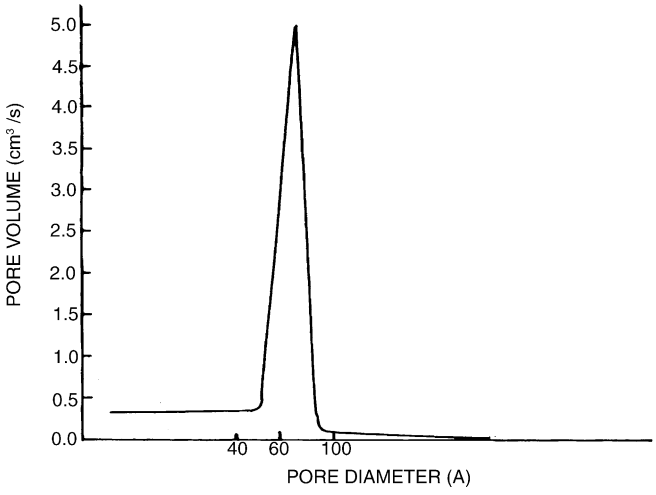

Fig. 1. Pore size distribution of SBA-15.

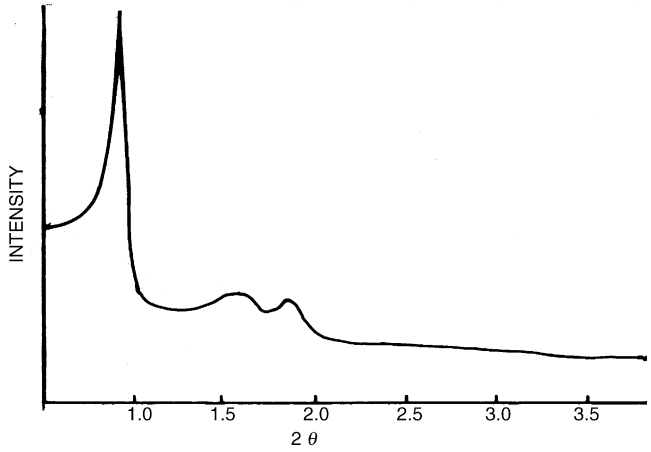

Fig. 2. X-ray diffractograms of SBA-15.

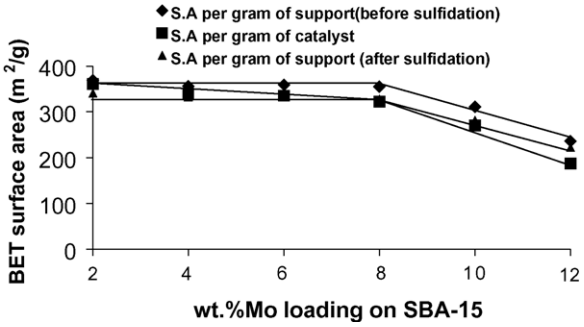

Fig. 3. Variation of surface area per gram of support (before and after sulfidation) and per gram of catalyst as a function of Mo loading.

oxygen chemisorption. The surface area results as a function of Mo loading are shown in Table 1. The BET area per gram of catalyst and per gram of support is shown in Fig. 3. It can be seen that BET area per gram of support remains more or less constant up to 8 wt.% Mo and then decreases. Similar behavior can also be seen after sulfiding. It is possible to extract information about monolayer formation from the surface area data. Normally when monolayer formation is taking place the BET surface area per gram of catalyst decreases, whereas BET surface area per gram of support remains more or less constant as a function of Mo content. As can be seen from Fig. 3, the invariance of BET surface area as a function of Mo content up to 8 wt.% suggests that the monolayer formation on this support takes place at 8 wt.% Mo. Similar behavior is obtained after sulfidation indicates that the monolayer is more or less intact after sulfidation. The support used here is mesostructured silica, it is interesting to compare the same with amorphous silica. In amorphous silica the monolayer formation takes place ~4 wt.% Mo (Table 2), whereas on mesostructured silica the monolayer formation takes place at 8 wt.% Mo. It appears that mesoporous silica accommodates higher amount of highly dispersed molybdenum than amorphous SiO_2. This observation suggests that the surface properties of mesoporous silica are different from amorphous silica. Therefore, surface area analysis suggests that the Mo monolayer formation takes place at 8 wt.% Mo and this monolayer is intact after sulfidation. It can also be inferred that the surface behavior of mesostructured silica is different from that of amorphous silica.

3.2.2. X-ray diffraction

Various catalysts containing different amount of Mo supported on SBA-15 were examined by X-ray diffraction in the region, where MoO_3 peaks appears. The diffractograms of the catalyst with different Mo loading are shown in Fig. 4. It can be noted that at initial loadings a broad peak centered around 20 Å–30 Å characteristic of siliceous materials, is only seen up to 8 wt.% Mo. It can be seen that weak signals due to Mo appears around 8% Mo and these signal intensity increases at higher Mo loadings. It is important to note that there is no indication for presence of molybdenum oxide below 8 wt.% Mo which suggests that MoO_3 is well dispersed on SBA-15 up to 8 wt.% Mo and at higher loadings evidence for the presence of crystalline MoO_3 can be seen. The absence of XRD signals indicated that the particle size of MoO_3 is smaller than ~40 Å up to 8 wt.% Mo and beyond this loading the crystallite size is higher. The X-ray results therefore suggests that MoO_3 is well dispersed up to 8 wt.% Mo loading and probably present as a monolayer up to this loading, and beyond this loading MoO_3 dispersion is poor. These results agree with the surface area analysis results which suggest that MoO_3 is well dispersed in the oxide state up to 8 wt.% Mo loading.

Table 1
BET surface area and oxygen chemisorption data of MoS_2/SBA-15 catalysts

Mo (wt.%)	BET surface area (m^2/g)	Oxygen uptake (μmol/g cat.)	O/Mo × 100	EMSA (m^2/g)[a]	%surface coverage(θ)[b]	Crystallite size (Å)[c]
2	361	26.9	25.8	15.2	4.22	13.7
4	340	37.4	17.9	21.1	6.22	19.7
6	335	47.6	15.2	26.9	8.05	23.2
8	322	62.2	14.9	35.2	10.93	23.6
10	270	49.6	9.5	28.0	10.40	37.1
12	187	43.7	6.9	24.7	13.22	50.5

[a] EMSA (equivalent MoS_2 area), calculated using a factor 0.56616 obtained from pure MoS_2 BET surface area divided by oxygen uptake.
[b] (EMSA/BET surface area) × 100.
[c] $5 \times 10^4/\rho M$, where ρ is the density of MoS_2 (4.8 g/cm^3) and M is EMSA/g of MoS_2.

Table 2
Characterization and catalytic activity of supported Mo, Ni, and Co promoted catalysts

Supported catalysts	BET surface area (m^2/g)	Oxygen uptake (μmol/g cat.)	Reaction rates (mol/h/g cat.) 10^{-3}	
			HDS	HYD
8% Mo/SBA-15	322	62.2	24.0	25.7
1% Co 8% Mo/SBA-15	275	67.0	34.2	36.8
3% Co 8% Mo/SBA-15	222	88.4	49.1	41.2
5% Co 8% Mo/SBA-15	195	52.2	27.5	27.5
1% Ni 8% Mo/SBA-15	263	65.0	26.9	25.5
3% Ni 8% Mo/SBA-15	212	72.6	39.6	32.5
5% Ni 8% Mo/SBA-15	185	58.7	32.7	10.7
8% Mo/γ-Al_2O_3	204	22.1	11.2	25.4
3% Co 8% Mo/γ-Al_2O_3	138	31.8	26.8	24.7
3% Ni 8% Mo/γ-Al_2O_3	141	29.0	19.1	29.1
2% Mo/SiO_2[a]	348	13.0	2.3	7.1
4% Mo/SiO_2[a]	340	27.1	5.6	17.0
6% Mo/SiO_2[a]	330	25.0	4.1	8.3
8% Mo/SiO_2[a]	324	23.6	4.0	6.5
3% Co 4% Mo/SiO_2[a]	–	–	11.8	60.0
3% Ni 4% Mo/SiO_2[a]	–	–	10.6	69.7

[a] Amorphous silica (S.A. 352 m^2/g).

3.2.3. Oxygen chemisorption

The oxygen uptakes were evaluated at −78 °C on samples sulfided at 400 °C. These results are shown in Table 1 and Fig. 5. It can be seen from the Table 1 that oxygen uptakes increase with Mo loading up to 8 wt.% Mo and beyond this loading there is decrease in oxygen uptake. From the oxygen uptake data several useful parameters such as O/Mo, equivalent Molybdenum sulfide area [EMSA], surface coverage by Molybdenum sulfide and its crystallite size can be calculated. These data as a function of Mo loading are shown in Table 1. The O/Mo which is a measure of dispersion of MoS_2 remains more or less constant up to 8 wt.% Mo and decreases at higher Mo loadings. The surface coverage by MoS_2 increases continuously up to 12 wt.% Mo but the surface coverage is low and is ∼13% of the BET surface of the catalyst. This observation suggests that Mo selectively interacts with small portion of the SBA-15 support surface. It is well known that oxide surfaces terminate with hydroxyl groups and some such hydroxyl groups of suitable strength and energy are involved in fixing the molybdenum [32]. These hydroxyl groups with suitable strength and energy are expected distributed randomly as small monolayer patches of average crystallite size calculated from oxygen chemisorption. It can be noted that the crystallite size increases beyond 8 wt.% Mo loadings. Comparing with XRD data on MoO_3/SBA-15 oxide precursors it appears that MoO_3 redisperses during sulfiding. The variation of oxygen uptakes with Mo loading suggests that in the sulfided state also the patchy monolayer formation is complete around 8 wt.% Mo loading.

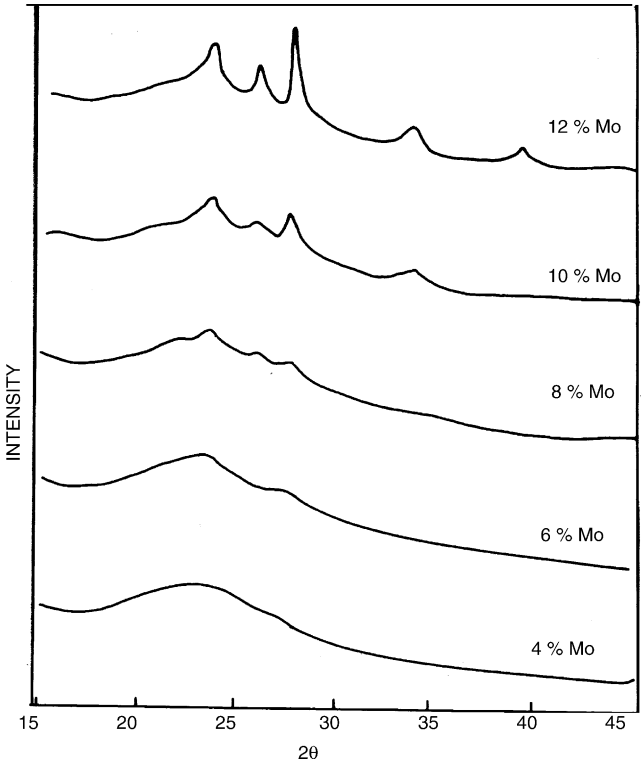

Fig. 4. XRD patterns of Mo/SBA-15 catalysts as a function of Mo loading.

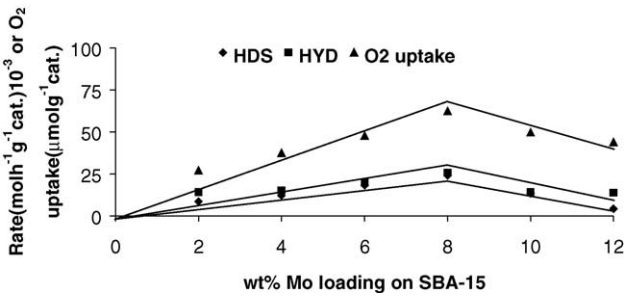

Fig. 5. Variation of oxygen uptake and catalytic activity with Mo loading.

3.2.4. Catalytic activity studies

The catalytic activities for HDS of thiophene and hydrogenation of cyclohexene as a function of Mo loading are shown in Fig. 5. It can be seen that the catalytic activities for both hydrogenation and hydrodesulfurization increase up to 8 wt.% Mo and decreases at higher loadings. It is interesting to compare HDS and HYD activity variation as a function of Mo loading with the behavior of oxygen uptake. It can be noted that both the functionalities and oxygen uptake increase up to 8 wt.% Mo and decrease beyond that loading. Such a behavior suggests that oxygen chemisorption correlates well with catalytic activities for both HDS and HYD. Since oxygen chemisorption correlates with both the functionalities and it is not specific to any one of the functionalities but measures general state of dispersion of MoS_2. It is well known that oxygen chemisorbs on anion vacancies and also it is generally agreed that HDS and HYD activities takes place on catalytic sites that include anion vacancies [24]. Therefore, it is not surprising that a correlation exists between the two characteristics of the catalyst.

3.2.5. Promotional effects

The catalytic activities of Co- and Ni-promoted Mo/SBA-15 are presented in Table 2. The promoter content is varied between 1 wt.% and 5 wt.% in case of both cobalt and nickel. It can be seen that the catalytic activities increases with promoter content up to 3 wt.% both in the case of cobalt and nickel, in case of hydrodesulfurization. Similar behavior is observed in the case of hydrogenation functionality also. Oxygen chemisorption on the promoted catalysts is shown in the same Table 2. It can be seen that oxygen uptakes and catalytic activities for HYD and HDS show similar behavior with respect to promoter content. Probably this is due to the fact that Co- or Ni-promoter contributes to increase in anion vacancies, which are connected with oxygen chemisorption and catalytic sites.

In the same Table 2, HDS and HYD catalytic activity data for laboratory prepared γ-Al_2O_3-supported Mo, CoMo, NiMo catalysts prepared in identical manner is presented for comparison purposes. It can be seen that SBA-15 supported catalysts are 2–2.5 times more active compared to γ-Al_2O_3-supported catalysts for both HDS and HYD activities. The activities and oxygen uptakes shown in bar graph in Fig. 6 indicates that activity increase in the case of SBA-15 supported catalysts is due to increase in dispersion of MoS_2 represented by the oxygen uptake.

At this stage it is necessary to summarize the characterization results and activity data and promotional effects and discuss further in order to understand molybdenum monolayer formation on SBA-15 and relationship between oxygen chemisorption and catalytic activities. The analysis of surface area variation as a function of Mo loadings indicated that the surface area per gram of support remains constant up to 8 wt.% Mo both in the case of oxidic and sulfidic states. Suggesting that molybdenum is well

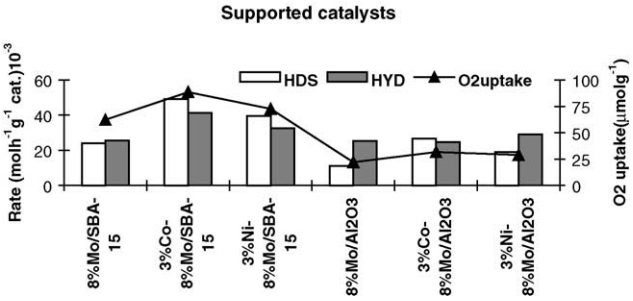

Fig. 6. Catalytic activities of Mo, CoMo, NiMo catalysts prepared using SBA-15 and γ-Al_2O_3 supports.

dispersed up to 8 wt.% probably as monolayer. XRD results indicated that up to 8 wt.% Mo, molybdenum oxide crystallite size is smaller than ~40 Å, which means that molybdenum is in a finely dispersed form up to 8 wt.%. Both these measurements suggested crystallite growth beyond 8 wt.% Mo in the oxidic state. Oxygen chemisorption was evaluated on sulfided catalysts, therefore this information pertains to sulfided state. The oxygen uptakes increase up to 8 wt.% Mo and then decreases at higher loadings. The MoS_2 crystallite sizes evaluated using oxygen chemisorption and O/Mo ratios suggest that in the so called monolayer region (2 wt.%–8 wt.% Mo) the crystallites are small and show less variation. O/Mo which is a measure of Mo dispersion is more or less constant in the same region. The coverage of SBA-15 surface by MoS_2 is small indicating that MoS_2 selectively interacts with specific regions of SBA-15 surface. Since the crystallite size is small it appears that MoS_2 on this support is of monolayer dimensions up to 8 wt.% Mo loadings in the sulfided state. The monolayer does not appears to be continuous but in the form of monolayer patches on SBA-15 surface. This can be understood through literature available on Mo interaction with inorganic oxide supports [32]. It is well known that molybdenum interacts with surface hydroxyl groups on supports like γ-Al_2O_3, MgO, TiO_2, SiO_2, etc. [33]. Only basic hydroxyl groups of suitable energy and strength participate in molybdenum anchoring [32,34]. These hydroxyl groups and their location on SBA-15 surface determines the molybdenum monolayer formation. Since the hydroxyl distribution is likely to be random, the interacted MoS_2 monolayer patches are expected to be randomly distributed.

The catalytic activites evaluated on sulfided catalysts for HDS and HYD increase up to 8 wt.% Mo and then decreases similar to oxygen chemisorption on the catalysts sulfided in similar manner. The parallel variation of catalytic activities suggests that the anion vacancies on which oxygen chemisorbs increase in number on the monolayer patches up to 8 wt.% Mo beyond which MoS_2 crystallite growth occurs as the hydroxyl groups of suitable energy and strength are no longer available on the SBA-15 surface beyond 8 wt.% Mo loading resulting in three dimensional crystallite growth of MoS_2. It appears that MoO_3 monolayer

patches are formed in the oxidic state is retained in sulfided state in the form of MoS_2 patches of monolayer dimensions. The number of these patches increase up to 8 wt.% Mo which contribute to the increase in anion vacancies at the edges of MoS_2. These anion vacancies also contribute to the activity, being a part of the active site; the activity also varies in a similar manner.

4. Conclusion

Ordered mesoporous SBA-15 suitable as support to hydrotreating catalyst is prepared by known procedures and used to prepare Mo, CoMo, and NiMo catalysts. The catalytic activities and oxygen chemisorption evaluated in sulfided state indicated that the formation patchy monolayer of MoS_2 on the surface is complete around 8 wt.% and three dimensional crystallite growth is inferred from calculated crystallite sizes at higher loadings. These results agreed with surface area analysis and XRD results obtained in the oxide state. The catalytic activities correlated well with the oxygen chemisorption. The oxygen chemisorption results suggested a patchy monolayer formation. A comparison with γ-Al_2O_3-supported catalysts clearly indicated that SBA-15-supported catalysts show superior activities compared γ-Al_2O_3-supported catalysts prepared in similar manner. The data presented for SiO_2-supported catalysts suggest that the surface of SBA-15, a mesostructured SiO_2 is different from amorphous silica with respect to molybdenum interaction and hydrotreating functionalities.

Acknowledgments

The authors are greatful to Director, Indian Institute of Petroleum, Dehradun for his encouragement and Mr. Muthu Kumaran thanks CSIR, India for a Junior Research Fellowship.

References

[1] Fuel Processing for Fuel Cell Applications, Special Issue of Catal. Today, in Saikatikaneni, A. M. Gaffrey, C. Song (Eds.), Catal. Today 77 (2002) and papers there in.
[2] C. Song, Catal. Today 77 (2002) 17.
[3] S.K. Maity, B.N. Srinivas, V.V.D.N. Prasad, A. Singh, G. Murali Dhar, T.S.R. Prasada Rao, in: T.S.R., Prasada Rao, G., Murali Dhar, (Eds.), Recent Advances in Basic and Applied Aspects of Industrial catalysis, Stud. Surf. Sci. Catal. 113 (1998) 579.
[4] T. Halachev, R. Nava, L. Dimitrov, Appl. Catal. A: Gen. 169 (1998) 111.
[5] T. Halachev, J.A. de los Reyes, C. Aranjo, G. Cordoba, L. Dimitrov, in: B. Delmon, G.F. Froment, P. Grange (Eds.), Hydrotreatment and hydrocracking of oil fractions, Stud. Surf. Sci. Catal. 127 (1999) 401.
[6] G. Murali Dhar, F.E. Massoth, J. Shabtai, J. Catal. 85 (1994) 44.
[7] S.K. Maity, M.S. Rana, S.K. Bej, J. Ancheyta Jiuarez, G. Murali Dhar, T.S.R. Prasada Rao, Appl. Catal. 205 (2001) 215.
[8] S.K. Maity, M.S. Rana, B.N. Srinivas, G. Murali Dhar, S.K. Bej, T.S.R. Prasada Rao, J. Mol. Catal. A: Chem. 153 (1/2) (2000) 121.
[9] G. Murali Dhar, H. Ramakrishna, T.S.R. Prasada Rao, Catal. Lett. 22 (1993) 351.
[10] R. Prins, V.J.H. de Beer, G.A. Somsserjai, Catal. Rev. Sci. Eng. 31 (1989) 1.
[11] F.E. Massoth, G. Murali Dhar, J. Shabtai, J. Catal. 85 (1994) 52.
[12] M.S. Rana, B.N. Srinivas, S.K. Maity, G. Murali Dhar, T.S.R. Prasada Rao, in: B. Delmon, G.F. Froment, P. Grange (Eds.), Hydrotreatment and Hydrocracking of oil fractions, Stud. Surf. Sci. Catal. 127 (1999) 397.
[13] M.S. Rana, B.N. Srinivas, S.K. Maity, G. Murali Dhar, T.S.R. Prasada Rao, J. Catal. 195 (2000) 31.
[14] F.P. Daly, H. Ando, J.L. Schmitt, E.A. Sturm, J. Catal. 108 (1987) 401.
[15] W. Zhaobin, X. Qin, G. Xiexian, E.L. Sham, P. Grange, B. Delmon, Appl. Catal. 63 (1990) 305.
[16] W. Zhaobin, X. Qin, G. Xiexian, E.L. Sham, P. Grange, B. Delmon, Appl. Catal. 75 (1991) 179.
[17] C. Pophal, F. Kameda, K. Hoshino, S. Yoshinaka, K. Segawa, Catal. Today 39 (1997) 21.
[18] K. Segawa, S. Sato, in: B. Delmon, G.F. Forment, P. Grange (Eds.), Hydrotreatment and hydrocracking of oil fractions, Stud. Surf. Sci. Catal. 127 (1992) 129.
[19] G. Murali Dhar, B.N. Srinivas, M.S. Rana, M. Kumar, S.K. Maity, Catal. Today 86 (2003) 45.
[20] T. Klimova, M. Calderon, J. Ramirez, Appl. Catal. A: Gen. 240 (2003) 29.
[21] A. Wang, Y. Wang, T. Kabe, Y. Chen, A. Ishihava, W. Qian, P. Yao, J. Catal. 210 (2002) 319.
[22] A. Wang, Y. Wang, T. Kabe, Y. Chen, A. Ishihara, W. Qian, J. Catal. 199 (2001) 19.
[23] U.T. Turaga, C. Song, Catal. Today 86 (2003) 129.
[24] T. Chiranjeevi, P. Kumar, M.S. Rana, G. Murali Dhar, T.S.R. Prasada Rao, J. Mol. Catal. A: Chem. 181 (2002) 109.
[25] L. Vradman, M.V. Landan, M. Herskowitz, V. Ezersky, M. Talianka, S. Nikitenko, Y. Koltypin, A. Gedanken, J. Catal. 213 (2003) 163.
[26] L. Kaluza, M. Zdrazil, N. Zilkova, J. Cejka, Catal. Commun. 3 (2002) 151.
[27] C. Song, K.M. Reddy, Prep. Am. Chem. Soc. Div. Petro. Chem. 41 (1996) 567.
[28] T. Chiranjeevi, P. Kumar, S.K. Maity, M.S. Rana, G. Murali Dhar, T.S.R. Prasada Rao, Micropor. Mesopor. Mater. 44–45 (2001) 547.
[29] D. Zhao, Q. Huo, J. Feng, B.F. Chmelka, G.D. Stucky, J. Am. Chem. Soc. 120 (1998) 6024.
[30] B.S. Parekh, S.W. Weller, J. Catal. 47 (1977) 100.
[31] K.S.P. Rao, H. Ramakrishna, G. Murali Dhar, J. Catal. 133 (1992) 146.
[32] H.-P. Boehm, H. Knozinger, in: J.R. Anderson, M. Boudart (Eds.), Catalysis Science and Technology, vol. 4, Springer, New York, 1983.
[33] H. Topsoe, B.S. Clausen, F.E. Massoth, in: J.R. Anderson, M. Boudart (Eds.), Hydrotreating Catalysis Science and Technology, vol. 11, Springer, New York, 1996.
[34] N. Yamagata, Y. Owada, S. Okazaki, K. Tanabe, J. Catal. 47 (1977) 358–363.